Published in "The Analysis of Emission Lines", eds. R. E. Williams and M. Livio, Space Telescope Science Institute Symposium Series 8, 1995

INFRARED EMISSION LINES AS PROBES OF GASEOUS NEBULAE

Harriet L. Dinerstein

Astronomy Department, University of Texas at Austin, Austin, TX 78712

Abstract. Infrared emission lines are just coming into their own as diagnostic tools for the study of gaseous nebulae. Various infrared line ratios provide the means to determine physical parameters such as extinction, density, temperature, and ionic and elemental abundances. In certain regimes, infrared lines provide essentially the *only* opportunity for determining these parameters, or even for detecting the gas. Examples include regions of high extinction, low temperature, and predominantly neutral material. I review the general properties of infrared emission lines and their characteristics as nebular diagnostics, and cite a number of illustrative applications. The latter are drawn from a wide range of fields, including star formation and H II regions, planetary nebulae, nova and supernova remnants, shocked and photodissociated gas, and AGN and starburst galaxies.

Table of Contents

- INTRODUCTION
- GAS DIAGNOSTICS
  - Extinction (A_V)
  - Electron density (n_e)
  - Electron Temperature (T_e)
- IONIZATION AND EXCITATION MECHANISMS
  - Photoionization: Characterizing the UV radiation field
  - Photodissocation regions
  - Shocks
- ABUNDANCES
  - Optically "invisible" gas
  - Ionic abundance ratios
  - Altered & evolving abundances
- SOME CURRENT ISSUES: A SAMPLER
  - The origin of strong [Fe II] lines
  - Curiosities at the Galactic Center
  - Infrared spectroscopy of AGN
- CONCLUDING REMARKS
- REFERENCES

1. INTRODUCTION

The phrase "infrared emission lines," like so many other topics covered at this meeting, is extremely broad. Therefore I will begin by defining and limiting the scope of this review. I will discuss only lines that arise from gas-phase atoms, ions, and molecules, and will not include spectral features produced by interstellar dust. In this review, "infrared" will mean the spectral region 1-200 μm, which corresponds to certain types of astronomical detectors; shorter wavelengths will be called "far red" (with apologies to Don Osterbrock), and longer wavelengths, "submillimeter." Another boundary condition is that I will restrict myself to low densities $n \leq 10^8$ cm^{-3}. Apart from these constraints, I will attempt to be as general as possible, though with no pretentions to completeness. This review is organized by physical properties and methods of analysis, rather than by class of

astronomical object. In selecting applications I have tried to sample diverse areas of astronomy, in order to illustrate the breadth and power of the various methods for measuring and constraining astrophysically interesting parameters.

One might begin by asking "why infrared?" Perhaps it is not quite as necessary to raise this question as it was a decade or two ago, when infrared instrumentation was relatively primitive, and one needed to justify the extra effort required to make observations in the infrared region. However, it remains true that infrared emission lines have a number of special characteristics that translate into distinctive advantages, and a few limitations. Some special qualities of infrared emission lines include: (1) access to regions with high visual extinctions; (2) avoidance of the temperature sensitivity that is essentially intrinsic to most optical and ultraviolet emission (hereafter, optical/uv) lines; and (3) and the ability to sample species that lack observable lines in the optical/uv, either because of the vagaries of atomic structure or because the gas is too cool to emit in lines from high energy levels.

Most of the observed infrared lines (other than recombination lines of H and He) connect fine-structure levels within ground state p^n configurations of abundant ions (where n is an integer between 1 and 5). A good synopsis of the physics of fine-structure lines can be found in Simpson (1975), an influential paper in the 1970's, a period of rapid advances in infrared spectroscopy. Other discussions of these lines can be found in Aller (1984, ch. 5), Watson (1985), and Osterbrock (1989, chs. 3 and 5). What follows here are just a few general points.

The upper levels of the fine-structure lines are populated by collisions, usually with electrons. For upper levels with small excitation energies χ, the populations are substantial. Whereas the excitation energies of the optical/uv lines are larger than the typical energy of the free electrons, for the infrared lines $\chi = h\nu << kT$ and the exponential term is nearly equal to unity. The ratio of populations of an excited level (1) to the ground level (0) in a two-level atom is

$$\frac{n_1}{n_0} = \frac{n_e q_{01}}{A_{10}} \left[1 + \left(1 + \frac{n_e q_{10}}{A_{10}} \right)^{-1} \right]; \quad q_{01} \propto \Omega(T) T^{-0.5} e^{-\chi/kT} \approx \Omega(T) T^{-0.5} \qquad (1.1)$$

(after Osterbrock 1989, eq. 3.25), where A_{10} is the radiative transition probability, q_{01} and q_{10} are the collisional excitation and de-excitation probabilities respectively, and $\omega(T)$ is the "collision strength," which depends only weakly on temperature. For lines in which both levels belong to the same electronic configuration, downward radiative transitions are forbidden by electric dipole selection rules. Combined with their low frequencies, this yields low transition probabilities, $A_{10} \leq 10^{-2}$ s^{-1}, for the fine-structure lines. However, the large populations of these levels tend to compensate for the low A values, making the net volume emissivities of the infrared lines (in energy units) comparable to those of the optical/uv lines, which arise from much smaller populations in higher-energy levels.

From equation 1.1 one can see that the small excitation energies of the infrared lines insure a weak dependence of the emergent line strengths on electron temperature T_e compared to the optical/uv lines. This has both advantages and disadvantages: it is helpful for deducing ionic abundances, since one need not know the exact value of T_e; however, such lines therefore give no information about the temperature. The low transition probabilities, combined with high collisional de-excitation rates, lead to small critical densities, where, for level i,

$$n_{\rm crit}(i) = \sum_{j<i} A_{ij} / \sum_{j \neq 1} q_{ij} \qquad (1.2)$$

(Osterbrock, eq. 3.31). As a result, the infrared lines are sensitive to density and clumping (i.e., Rubin 1989). They are good density indicators for low-density regions, but "saturate" to asymptotic values at relatively low densities, whereupon they become good mass tracers.

The history of the observations of the infrared emission lines more or less begins in the 1970's, when these lines were first observed in bright, compact H II regions and planetary nebulae. By 1982, the list of detected lines ran to fifteen (e.g., Dinerstein 1983). In the 1980's infrared lines began to be observed from a more diverse group of sources, such as novae, supernovae and supernova remnants, and photodissociation regions. Within the last few years, there has been a rapid growth in infrared spectroscopy of extragalactic sources, including active galactic nuclei and starburst galaxies. The fact that it is no longer feasible or sensible to present a comprehensive list of detected infrared emission lines in a review such as this one is a measure of the maturity of the field and the diversity of the astronomical sources and regions that benefit from being studied with infrared line spectroscopy.

2. GAS DIAGNOSTICS

The first step in the analysis of emission line strengths from nebulae is generally the derivation of physical parameters that characterize the local conditions in the gas, primarily density and temperature (see the synopsis of the standard or "conventional" analysis of H II regions, in Dinerstein 1990). This is as true for infrared lines as for optical/uv lines, and the specific methods used with infrared lines are essentially analogs of techniques developed for optical/uv lines.

2.1. Extinction (A_V)

Determination of the extinction towards the line-emitting material is a prerequisite to the derivation of other properties, since further analysis requires knowledge of the true line intensities, corrected for extinction. The usual approach is to measure the intensity ratios among lines whose intrinsic relative strengths are considered known. Discrepancies are ascribed to extinction, assumed to follow a particular law A(λ), and a best fit is found for the overall scaling factor, usually characterized by A_V or sometimes A_K (i.e., Mathis 1990). The most commonly used set of line ratios is the recombination spectrum of H I; this is called the *hydrogen decrement* method. In the optical, one uses the Balmer lines (e.g., Hβ / Hα, Hγ / Hα), whose relative intensities in the absence of extinction are known to high accuracy and have little dependence on temperature or density (Osterbrock 1989, ch. 4.2). The main transitions used in the infrared are the Paschen and Brackett series, which extend out to 4.05 μm (Br α). These lines are used to determine extinctions to H II regions in our own Galaxy, and in other galaxies (e.g., Lester et al. 1990). A couple of caveats should be kept in mind, however. First, where the geometry is complex and the observations integrate over material with a range of A_V values, the effective extinction law may have a form quite different from the standard one, and may have to be determined empirically by sampling lines at various wavelengths and interpolating (i.e., Lester, Dinerstein, & Rank 1979). Second, there are situations, such as high densities and high optical depths, where the intrinsic recombination decrement deviates strongly from the classic "Case B" values. Examples of the latter range from the "line excess" problem in young stellar objects (Thompson 1982; Natta et al. 1988), to broad lines in active galactic nuclei (Kawara, Nishida, & Phillips 1989; Goodrich 1990).

When H I recombination lines are not available, one can use pairs or sets of lines with different wavelengths that arise from the same upper level of any species. An early example of this method was a comparison the strengths of [S II] lines near 1 μm with others near 4000 Å (Fig. 1) to determine the extinction towards the metal-rich knots in the Cas A supernova remnant (Searle 1971); these knots are composed entirely of heavy elements and contain no H or He at all. To determine extinctions towards regions where hydrogen is molecular, it is common to use H_2 quadrupole lines from common upper levels; applications include the shocked gas in Orion (e.g., Geballe et al. 1986) and the evolved bipolar nebula GL 618 (Latter et al. 1992). The rich energy level structure of Fe II (Nussbaumer & Storey 1988) provides a multitude of line ratios to use in partially ionized regions such supernova remnants (see Fig. 1).

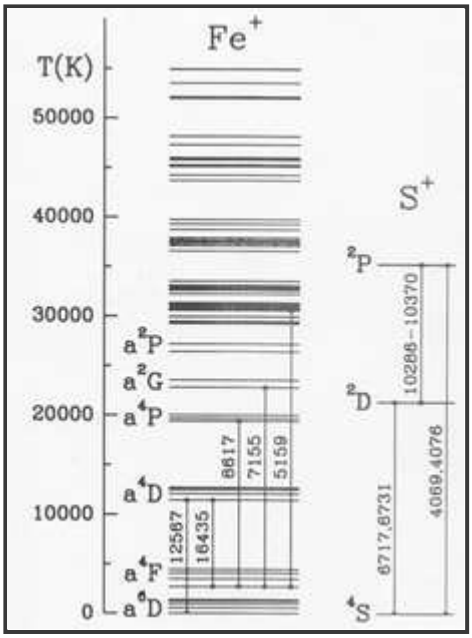

Figure 1. Energy levels of Fe II & S II. (From Oliva, Moorwood, & Danziger 1991)

2.2. Electron density (n_e)

The honorees of this conference were among the pioneers in using optical line intensity ratios to deduce densities in ionized nebulae (Seaton & Osterbrock 1957; updated in Fig. 5 of Osterbrock 1988). Intensity ratios of pairs of infrared lines can similarly be used to infer gas densities. A comprehensive discussion of infrared density indicators is given by Rubin (1989). The critical densities of the infrared lines fall mostly in the range 10^2 cm^{-3} < n_{crit} < 10^6 cm^{-3}, with a general tendency of the longer-wavelength lines to have lower values than shorter-wavelength lines because of their lower *A* values (equation 1.2). For example, log n_{crit}([O III] 51.8, 88.4 μm) (3.5, 2.7), while log n_{crit}([N II] 122, 204 μm) = (2.4, 1.6). On the other hand, the critical densities of [S III] 18.7, 33.5 μm are higher than those of some optical lines (see Fig. 2). These three pairs of lines have been used extensively to study obscured Galactic H II regions (e.g., Moorwood et al. 1980; Colgan et al. 1993). Ratios of infrared to optical lines can also be used as density indicators (e.g., Keenan & Conlon 1993).

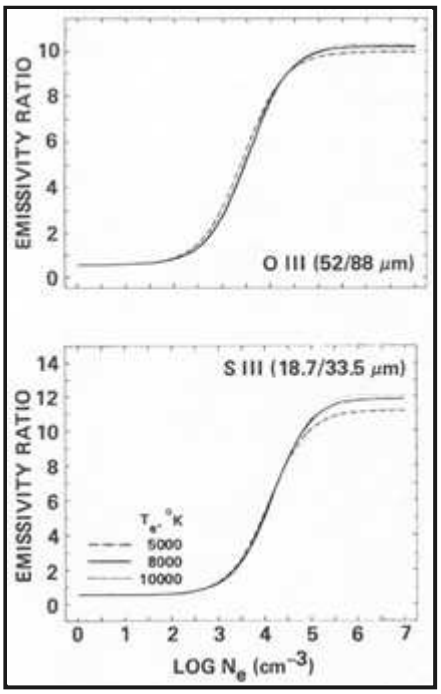

Figure 2. [O III], [S III] lines as n_e diagnostics. (From Rubin 1989)

In partially ionized regions where the gas is heated by shocks and/or by photoelectrons donated by species such as C^+, Si+ and Fe^+, local gas densities can be derived from ratios of [Fe II] lines. This species provides a multitude of strong emission lines in the infrared, particularly between 1.25 μm and 1.9 μm, from which density-sensitive ratios can be formed (Nussbaumer & Storey 1988). Most of these [Fe II] ratios are useful density indicators at relatively high densities, 10^4 < *n* < $10^{5.5}$ cm^{-3} (e.g., Oliva, Moorwood, & Danziger 1989).

Studies that have measured densities from more than one pair of infrared lines often find that different indicators yield different nominal values of n_e. This should not come as a surprise. It behooves us to bear in mind the complexity of real nebulae and the limitations of diagnostics:

"It must always be remembered that mean temperatures and densities derived from these diagnostic ratios are complicated averages over the structure of the nebula, weighted by the emission processes themselves. Thus the mean temperature is weighted toward high temperature, where the collisionally excited emission lines are all strongest, and the mean density is weighted toward the critical densities, where the emission 1s most efficient."

(Osterbrock 1988, p. 419). For ratios involving infrared lines only, temperature effects are minimal, but density is an important consideration. Nebulae are almost inevitably inhomogeneous, probably both on large and small scales, and diagnostics from lines with different critical densities will be biased accordingly. The effects of such biases can propagate further in the analysis. If the "wrong" (single-value) density is inferred, then the wrong emissivity will be used in the subsequent calculations, and an incorrect abundance will be derived. Rubin (1989) examined the effects of such "density bias" on ionic ratios, for several representative cases of inhomogeneous nebulae. He found that the errors in the derived abundance vary widely for different sets

of lines, ranging from negligible (e.g., < 10% for N^{++}/O^{++}) to significant (> 50% for several other ratios under reasonable conditions); his analysis also included many optical/uv line diagnostics.

2.3. Electron Temperature (T_e)

Electron temperatures (T_e) of ionized nebulae can be determined from intensity ratios of collisionally excited lines from levels of widely separated energies. The pre-eminent optical line indicator for T_e is the ratio of [O III] 4363 Å to one or both of the stronger [O III] lines at 4959, 5007 Å (e.g., Osterbrock 1989, Fig. 5.1; Dinerstein 1990). As pointed out in Section 1, infrared fine-structure lines are relatively insensitive to T_e. Thus, by themselves they are not useful for measuring T_e in typical hot, ionized nebulae; however, one can construct T_e diagnostics by comparing infrared lines from low-lying levels with optical/uv lines from higher-excitation levels. This can provide a means to derive T_e values for regions that lack optical/uv T_e diagnostics. For example, [Ne V] 24.3 μm can be combined with [Ne V] 3426Å, and [O II} 25.9 μm similarly with far-uv lines, to infer T_e for the high-ionization zones of planetary nebulae (Shure et al. 1983a, b; Rowlands et al. 1989). In regions that do not produce optical/uv emission lines, infrared line ratios can be used as temperature indicators in particular regimes, e.g., [O I] 145/63 μm at $T \leq 500$ K. However, because infrared lines are strongly affected by collisions at relatively low densities, their dependences on n and T are often difficult to separate. It may be necessary to measure at least two line ratios from one ion in order to derive meaningful constraints on T (Keenan, Burke, & Aggarwal 1991). In some cases it is necessary to combine lines from more than one species and assume a value for their relative abundances. For example, in photodissociation regions, [O I] 63, 145 μm and [C II] 157 μm can be used together to constrain n and T, at least in certain regimes (Fig. 3, from Watson 1985; also Tielens & Hollenbach 1985).

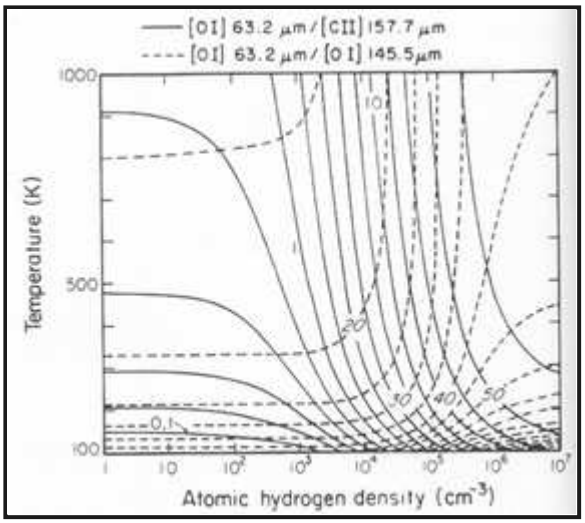

Figure 3. Mapping of the infrared [C II], [O I] line ratios to n and T. (From Watson 1985).

There is no reason to expect that real nebulae are isothermal. As was the case for density, observations will include emission from material at a range of temperatures, particularly if made with large apertures. The spread in temperatures is likely to be modest ($\leq$ 30%) compared to density inhomogeneities, which could cover several orders of magnitude. However, for optical/uv lines, with their exponential emissivity dependence on T_e, even modest T_e variations produce enormous changes in line strengths and inferred parameters. A formalism for characterizing the temperature distribution in non-isothermal nebulae was introduced by Peimbert (1967), who defined a mean temperature T_0 and an rms "temperature fluctuation parameter" t_2. These parameters can be related to, and therefore measured by, intensity ratios of lines with different temperature dependences (i.e., Peimbert & Costero 1969). If the spread in T_e is large, the use of a single T_e value (determined from the standard diagnostics) to determine ionic abundances can yield inaccurate results. A spread of just a few percent can lead to abundance errors of a factor of two or worse, for very temperature-sensitive lines!

The rich infrared-optical [O III] spectrum offers a particularly attractive opportunity to constrain and characterize the temperature properties of nebulae. The ground 3P term gives rise to the strong far-infrared lines at 52 and 88 μm that have already been discussed as density indicators, whereas the higher levels produce the traditional optical [O III] temperature diagnostic (Fig. 4). By combining observations of a single far-infrared line (e.g., 88 μm) with two optical lines, Dinerstein (1983) showed that it was possible to solve simultaneously for n_e and T_e from a single ion. In Dinerstein, Lester, & Werner

(1985, hereafter DLW), both far-infrared [O III] lines were compared with 5007 Å; the mapping of this ratio in the (n_e, T_e) plane is shown in Fig. 5. The latter technique has the advantage of providing a determination of T_e that is independent of the 4363/5007 Å line ratio, and is less weighted or "biased" by small amounts of high-temperature gas than the optical ratio. Indeed, if one can measure *four* [O III] lines in a particular nebula and therefore construct *three* diagnostic line ratios, it should be possible to extract a measure of the inhomogeneity of the gas in addition to "mean" values of n_e and T_e. As shown in DLW (Appendix), using Peimbert's (1967) formalism,

$$T_e(5007\ \text{Å}/52\ \mu\text{m}) \approx T_o \quad \text{and} \quad T_e(4363\ \text{Å}/5007\ \text{Å}) \approx T_o(1+3t^2) \qquad (2.3)$$

making it (in principle) straightforward to solve for values of both T_0 and t^2. The accuracy of this method, however, depends critically on one's ability to calibrate the absolute far-infrared fluxes correctly, since ratios are taken relative to optical line fluxes measured with completely different instrumentation and flux standards. DLW concluded that there was evidence for significant non-zero values of t^2 in four observed planetary nebulae, with an average value of about .06. Compensation for this degree of inhomogeneity would elevate the O/H abundance by nearly a factor of two. These values of t^2 are only slightly higher than recent values derived for several galactic H II regions from various optical indicators (Peimbert 1993 and references therein). However, new and better-calibrated measurements of the far-infrared lines in NGC 6543, formerly found by DLW to have $t^2 > 0.1$, suggest that the actual value is smaller (Dinerstein et al. 1995). The promise of this method, and implications for the nebular oxygen abundances, await a larger set of accurately calibrated far-infrared line fluxes for optically well-studied nebulae, which are likely to become available in the next few years, from airborne studies and from new infrared space observatories.

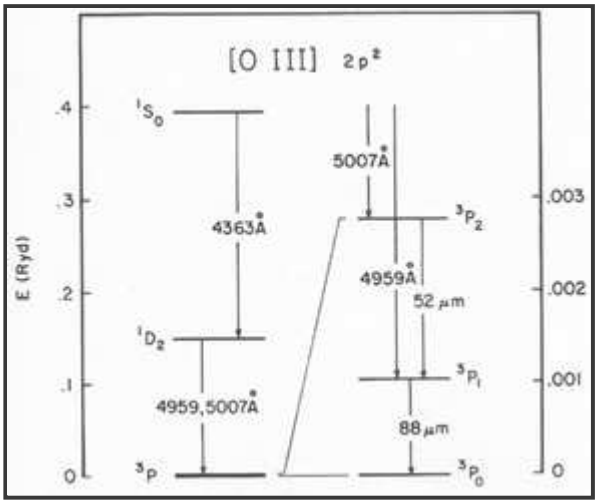

Figure 4. Energy level diagram for [O III]. (From Dinerstein, Lester, & Werner 1985.)

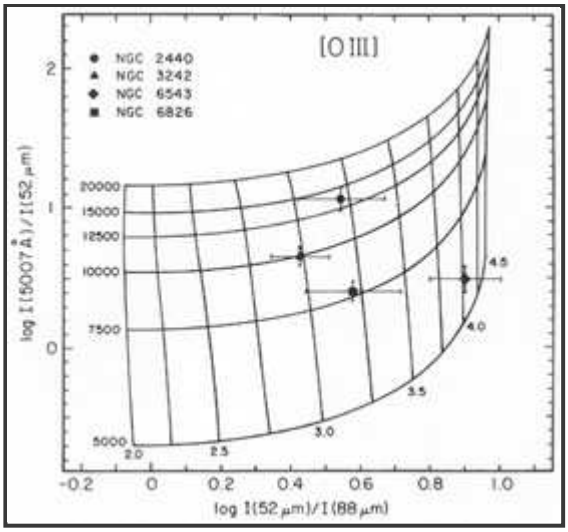

Figure 5. Infrared/optical [O III] diagnostics. (From Dinerstein, Lester, & Werner 1985.)

3. IONIZATION AND EXCITATION MECHANISMS

Further analysis of nebular emission lines can be categorized as falling in two areas: (1) determination of additional properties *intrinsic to the nebular gas*, such as elemental abundances, geometry, or total mass; or (2) derivation of properties of the *agents or mechanisms responsible* for ionizing and heating the gas, such as central star temperatures or shock velocities. To address the type of question, one must first decide what mechanism is responsible for the line emission; this determines the particular parameters to be evaluated. Knowledge of the excitation mechanism is often crucial to deriving meaningful results on quantitative properties of the gas as well.

3.1. Photoionization: Characterizing the UV radiation field

For photoionized nebulae, estimates of the surface temperatures of the central stars have long been made using observations of optical/uv emission lines from ions with different ionization windows. (By "window" I mean the range between the ionization potential of the next lower ionization state $\chi(X^{n-1})$, which is the minimum energy needed to create X^n, and $\chi(X^n)$, the energy it takes to ionize and thus destroy X^n.) In principle, the stellar temperatures can be calibrated empirically, from nebulae with central stars of known surface temperatures, but in practice this is rarely done. Instead, nebular ionization models are usually used at least to extend or interpolate such calibrations, and are often used as stand-alone calibrators. For example, mid-infrared spectra of obscured H II regions sample two strong ionic lines from species with very different lower bounds in χ: [Ne II] 12.8 μm (21.6-40.9 eV) and [S IV] 10.5 μm (34.8-40.7 eV). In H II regions ionized by normal thermal stellar spectra, the observed ratio of these two lines gives a first-order indication of the temperature of whether the central star (e.g., Rank et al. 1978).

When airborne or space infrared observations are available, a larger variety of ions may be sampled, and the application of detailed models is more fruitful. Sequences of model nebulae can be constructed specifically to fit observations of the infrared lines for a particular nebula (e.g., Simpson & Rubin 1984). While this may seem unnecessarily involved, nebular models developed for optical/uv observations have shown that the ionization balance in a nebula is significantly affected by nebular properties. One of the most critical is the local ratio of photons to atoms, or "ionization parameter;" changes in this parameter can mimic or mask changes in the stellar temperature (e.g., Evans & Dopita 1985). Ionization ratios formed from infrared lines are affected by the ionization parameter, the density structure and inhomogeneities, and internal non-gray opacity due to dust (Herter, Helfer, & Pipher 1983) or atoms (e.g., Rubin 1985). Geometry is another potentially important factor. Relaxing the assumption of spherical symmetry, for example in "blister" H II regions located on the edge of a dense cloud, changes the predicted ionization structure (Rubin et al. 1991). Thus, there is not always a unique correspondence between a particular observed line ratio and stellar temperature; determination of the latter will always require additional assumptions or constraints on the nebular structure.

A similar moral appears in the story of the He I 2.06 μm/H I(Br γ) 2.16 μm line ratio, which is relatively easy to observe in moderately obscured H II regions, and is therefore attractive as a possible indicator of ionizing star properties. It is well known that the ionic abundance ratio He^+ / H^+ varies with the surface temperature of the ionizing star (e.g., Osterbrock 1989, Fig. 2.5). However, this does not translate in a simple way into the variation of this particular line ratio, because the energy level structure of He I makes it prone to strong radiative-transfer effects (see Osterbrock 1989, Fig. 4.4). Indeed, the strength of the 2.06 μm

line is sensitive to nebular geometry, density, and velocity structure as well as to optical depth (Shields 1993). Other infrared He I lines do not suffer from as many problems, but are intrinsically weaker and hence more difficult to observe.

Geometry and density effects can only do so much; the presence of highly ionized species in a photoionized nebula requires a relatively hot source for the radiation field. Highly ionized species are often seen in the optical/uv spectra of planetary nebulae with particularly hot central stars; such nebulae are good places to look for infrared emission from ions of very high ionization potential, sometimes called "coronal lines." Examples include [Ne VI] 7.65 μm (Pottasch et al. 1985), [Si VI] 1.96 μm, and [Si VII] 2.48 μm (Ashley & Hyland 1988).

High ionization species are also found in the ejecta of recent classical nova events. Indeed, infrared coronal lines were first identified in a nova (Grasdalen & Joyce 1976). Since then it has been found that many, if not all, novae show high-ionization infrared lines such as [Si VI], [Si VII], [Al XIII], [Ne VI], etc., starting about 10 to 300 days after visual maximum (see reviews by Gehrz 1988; Dinerstein & Benjamin 1993). The record-setting infrared line is [Si IX] 3.92, requiring 401 eV to produce (Greenhouse et al. 1990). The origin of the coronal ions has been controversial. Greenhouse et al. argue that they arise from gas in collisional ionization equilibrium at coronal temperatures. However, the observed near-infrared line-to-continuum ratios in several recent novae (Benjamin & Dinerstein 1990) support the view that the gas is thermally cool, and the coronal ions are produced through photoionization by the hard radiation field of the hot white dwarf (Williams 1991).

Novae also provide a fascinating opportunity to watch a nebular spectrum evolve, in response to the changing surface temperature of the white dwarf and declining density of the ejecta. During the first year or two after visual maximum, both of these effects drive the ionization balance towards higher ionization states. Figure 6 shows a particularly dramatic example of spectral evolution: Nova Cyg 1992 in the K-band during its transition to the "coronal" phase. If conditions in the ejecta can be properly modeled, the changing spectrum can be used to infer the spectral evolution of the white dwarf. The composition of the ejecta, which are enriched in metals due to the thermonuclear runaway and in some cases may also include material originating from the interior of the white dwarf, is also of interest (Section IV).

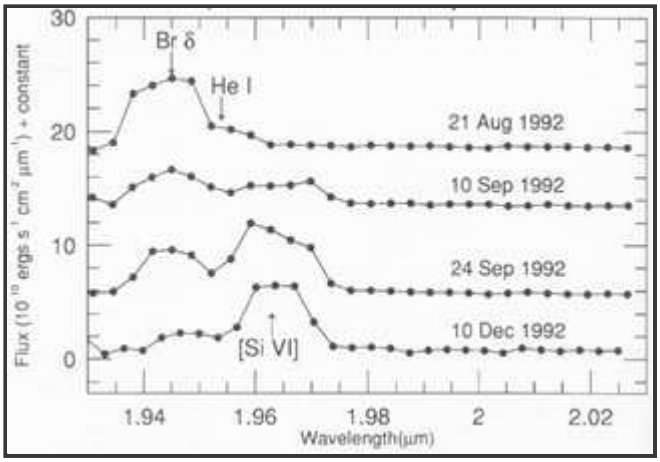

Figure 6. Evolution of the spectrum of N Cyg 1992 near 2.0 μm, during the transition to the "coronal phase." Note the declining strength of H I Br δ 1.94 μm and dramatically increasing strength of [Si VI] 1.96 μm on a timescale of a few weeks. (From Dinerstein & Benjamin 1993)

The presence of lines from species with a wide range in ionization potential is often taken as an indicator of ionization by a power-law continuum, for example from an active galactic nucleus (AGN). Several groups have predicted intensity ratios for infrared emission lines, for various models of AGN's, starburst galaxies, and other related objects (Voit 1992; Spinoglio & Malkan 1992). The idea is to construct diagnostic diagrams, by plotting pairs of line ratios against each other, in which these different types of regions can be easily separated and distinguished. The technique is similar to indicators based. on optical and far red lines developed by Baldwin et al. (1981) and Osterbrock, Tran, & Veilleux (1992) respectively. It has also been suggested that the intensities of some infrared coronal lines can be enhanced by laser effects in AGNs (Greenhouse et al. 1993).

3.2. Photodissocation regions

The collisionally excited emission lines in ionized nebulae are populated by interactions with free electrons that are produced by the photoionization of atoms, primarily hydrogen. Photons with energies slightly less than 13.6 eV penetrate somewhat farther, and dominate the energetics of the region just beyond the edge of the Strömgren sphere. The last decade has seen a dramatic

growth of interest in such transition regions between ionized nebulae and adjacent molecular clouds, where the gas is warm but mostly neutral. In these regions, the electrons are photoelectrons from grains, or from gaseous Species with ionization potentials lower than that of H, of which the most abundant is neutral atomic carbon. Models of these so-called "photodissociation regions" or PDRs (Tielens & Hollenbach 1985, hereafter TH) predict that their temperatures are of order $\approx$ 100-1000K, and that they cool primarily through infrared and submillimeter spectral lines. There are also significant H_2 populations in excited vibration-rotation levels in these regions.

The literature contains two types of theoretical studies of PDR's: those that focus on the details of the near-infrared H_2 quadrupole emission spectrum, and those that emphasize the energetics, chemistry, and longer-wavelength lines. The first type of model treats the populations of each excited H_2 vibrational-rotational level individually, in order to predict accurate intensities of observable emission lines (Black & van Dishoeck 1987; Steinberg & Dalgarno 1989). The two main mechanisms for populating these levels are collisions (as in a thermalized, shock-heated gas), and fluorescence or "uv-pumping." The latter operates by the absorption of uv photons (with 912 Å < λ < 1100 Å) which excite the molecules to higher electronic states, followed by a radiative cascade through the levels that give rise to the infrared lines. This process was discussed 20 years ago (i.e., Black & Dalgarno 1976), but not actually observed in the interstellar medium until 10 years later (Hayashi et al. 1985; Sellgren 1986). Both the absolute efficiency (line brightness per unit mass) and the relative line intensities of fluorescent H_2 emission are dramatically different from those of a thermalized, collisionally-excited spectrum. In particular, only a fluorescent spectrum will show significant emission in lines from high vibrational levels $v \geq 3$. Two examples of "pure" or "radiative" fluorescent regions are the reflection nebula NGC 2023 (Gatley et al. 1987) and the planetary nebula Hubble 12 (Dinerstein et al. 1988; Ramsay et al. 1993). However, if the illuminated material is sufficiently dense, the spectrum will be modified by collisional effects, which tend to thermalize the lowest-lying energy levels ($v \leq 2$) but not the higher vibrational states. This is called a "collisional fluorescent" spectrum by Steinberg & Dalgarno (1989). Another complicating factor is that gas illuminated by X-rays (a harder radiation field than that from ordinary hot stars) may also produce line ratios that are intermediate between the "pure" collisional and fluorescent cases (see article by A. Dalgarno in this volume).

Several techniques have been used to distinguish fluorescent excitation of the H_2 lines from emission produced entirely by collisions in shock-heated gas. One method that has been popular because of its simplicity and ease of measurement is to simply take the ratio of the v = 2-1 S(1) line at 2.247 μm to the v 1-0 S(1) line at 2.121 μm. These lines are sufficiently close in wavelength that they can be observed simultaneously with some instruments. Under typical collisional excitation conditions, this ratio is about 1/10; for fluorescence, it is about 1/2. However, this diagnostic is fallible; in particular, at densities approaching 10^4 cm^{-3} the v = 2 level may be depopulated by collisions, even if the original "pump" was uv radiation. A more sophisticated approach that requires additional data is to plot the data in a level-population vs. excitation energy diagram (e.g., Hasegawa et al. 1987). In such a diagram, collisionally populated levels will fall along a straight line defined by a single excitation temperature, or a smooth curve for a mixture of thermalized components with a range in temperature (a more realistic case for shocked gas). For a fluorescently excited gas, the vibration or rotation temperatures calculated from different pairs or sets of lines will have different slopes. The difference is illustrated in Fig. 7. A more efficient approach for simply detecting fluorescent emission (as opposed to studying its spectrum) is to observe lines arising from very high v levels, that are absent from a thermal spectrum (e.g., Luhman et al. 1994). Most of the strongest high-v lines, such as the v = 6-4 lines, fall in the J and H bands.

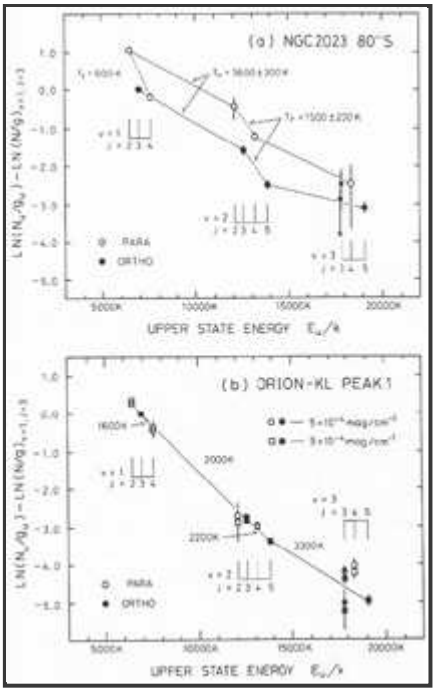

Figure 7. Population/excitation-energy diagrams for fluorescent H_2 emission (left), and for shock-excited emission (right). Note the disparate values of T_{vib} and T_{rot} for fluorescence, and the smooth slope of the thermalized gas. (From Hasegawa et al. 1987).

The second class of PDR models trace the chemistry, heating, and cooling of uv-irradiated molecular clouds, from the ionization front to deep into the cloud. The path length is specified either by N(H) or by A_V; the latter is closely related to the increasing extinction seen by the uv photons. Temperatures in these regions range from as high as 1000K to as low as 50K, depending on the physical conditions, and the strongest emission lines are the far-infrared fine-structure lines of [O I] and [C II]. These are the main cooling lines for atomic gas over a very wide range of physical conditions, approximately 20K < T < 2000K and 2 < log n < 6 (see Fig. 10 of TH). As discussed above, the intensity ratios among these lines are diagnostics of temperature and density (e.g., Fig. 3). The two key parameters of PDR models are the intensity of the uv radiation field, expressed in multiples of a "standard" interstellar intensity, denoted χ or $G = I_{UV} / I_{UV}(IS)$, and the gas density in. The model yields the run of temperature for given values of G and n. PDR models have been computed for conditions ranging from dense, clumpy media (Burton, Hollenbach, & Tielens 1990) to low-density extended gas in galaxies (Hollenbach, Takahashi, & Tielens 1991). The predictions of how the line intensity ratios map into parameters G and n have been applied to situations as diverse as galactic nuclei (Wolfire, Tielens, & Hollenbach 1990; Carnal et al. 1994) and planetary nebulae (Dinerstein et al. 1995b).

3.3. Shocks

The *ultimate* energy source for the collisionally excited emission lines in ionized nebulae and photodissociation regions is the radiation field, although collisions are the *proximate* cause of the line emission. An alternate heating mechanism is the mechanical action of interstellar shocks (supersonic compressions). Conditions in the "post-shock" region, the material that has already passed through the shock, depend on the shock velocity v_s and the "pre-shock density" n_0 (the initial density of the gas before it encounters the shock). These are the two primary parameters that are usually extracted from attempts to fit observations of shock-produced emission lines. The ionization, chemical, and thermal structures of the shock and post-shock zone are also affected by the magnetic field strength. Shocks are classified as "J-type" or "C-type" depending on whether there is a discontinuity or "jump" (J) in the gas properties at the interface, or a gradual or "continuous" (C) transition between the pine- and post-conditions (Draine 1980; McKee, Cheinnoff, & Hollenbach 1984). Recent reviews of the theory of interstellar shocks have been presented by Shull & Draine (1987) and Draine & McKee (1993).

Relatively slow shocks ($v_s \leq$ 50 km s^{-1}) moving into molecular clouds cool primarily through infrared and submillimeter lines of neutral and molecular species, such as [O I] 63, 145 μm, [C I] 370, 610 μm, and, at $v_s \geq$ 10 km s^{-1}, pure-rotation transitions

of H_2 (Draine, Roberge, & Dalgarno 1983). The relative strengths of the different lines vary with v_s, n_0, and the shock type and structure. Given a set of models, the shock parameters can be constrained by plotting the loci of observed line ratios in (v_s, n_0) phase space (e.g., Fig. 6 of McKee, Chernoff, & Hollenbach 1984). Faster shocks dissociate the H_2 molecules, produce a high-temperature zone that illuminates the pine-shock gas with uv radiation (the radiative "precursor"), and ionize some species (Hollenbach & McKee 1989). In such cases the H_2 molecules may re-form on the grain surfaces after the shock passes, and be released into the gas phase. When a number of different lines are observed, the level populations can be compared with the predictions of shock models in order to estimate the magnetic field strength and probe the detailed shock physics (e.g., Brand et al. 1988).

Supernova remnants (SNRs) are an obvious site of fast interstellar shocks. An interesting, still unsolved, puzzle is the extreme strength of the near-infrared [Fe II] lines in SNRs. This phenomenon was first noticed in IC 443, where the 1.64 μm [Fe II] line vastly outshines H I Br γ (Graham, Wright, & Longmore 1987). Indeed, the value of this ratio in SNRs exceeds its value in H II regions by a factor of about 500! The dilemma is: can the strength of the [Fe II] lines be explained entirely by the ionization structure of the post-shock region, or it is necessary to invoke grain destruction by the shock, liberating Fe atoms and thereby enhancing the gas-phase Fe abundance? A further complication is that strong [Fe II] emission may also be produced by photoionization by a power-law continuum, as in the Crab Nebula (Graham, Wright, & Longmore 1990), and possibly AGN (see Section V). Observations of multiple [Fe II] lines can constrain the physical conditions (Section II), and in combination with H_2 lines, may make it possible to distinguish among the different proposed mechanisms for enhancing the [Fe II] emission (Graham et al. 1991; Oliva, Moorwood, & Danziger 1991).

4. ABUNDANCES

Once one has information about the local physical conditions and understands the mechanism populating the particular emission lines observed in an object (e.g., collisions, radiative pumping, or - not discussed above - direct recombination or recombination cascades), it becomes possible to infer chemical abundances. Essentially, the amount of material required to produce the observed lines is given by the ratio of the line luminosity to the emissivity per ion (where these quantities are integrated over the angular size and along the line of sight). By taking ratios of pairs of lines, one avoids the need to know the source distance. In many cases, ratios enable one to at least partially cancel out the line emissivity dependences on n and T, yielding a relatively accurate value of the abundance ratio. This can be done directly (which is sometimes called an "empirical" determination), or by comparison with ionization structure models. The most elaborate procedure is to compile an extensive set of observed line fluxes, construct a specific model tailored to the particular source, and "tune" the model until the predictions match the observations in detail. Below I discuss some of the areas in which studies of infrared lines have contributed novel information. These include optically obscured sources, ions that have with no observable lines in the optical spectral region, and regions with temperatures so low that they emit only infrared and longer wavelength lines.

4.1. Optically "invisible" gas

As discussed in the Introduction, one of the drivers for observing the infrared spectral region is to study objects that are obscured by dust, whether internal to the object or in the foreground. One major domain of obscured regions is the entire inner disk of the Milky Way, including the Galactic Center region and virtually all H II regions at $R_{gal} \leq 5$ kpc. Although some information can be determined from radio line spectroscopy (including values for T_e, which is inversely correlated with the abundance of the main coolants), infrared spectroscopy is the most direct way to investigate properties of the ionizing stars and to assess global trends such as abundance gradients. Mid-infrared observations ($8 \leq \lambda \leq 25$ μm) are useful for studying S, Ar, and Ne, since more than one ion of each element is represented in this spectral region (e.g., Herter, Helfer, & Pipher 1983). Some of these lines, however, are inaccessible from the ground and require airborne platforms such as the KAO (Kuiper Airborne Observatory) or satellites (e.g., IRAS; Simpson & Rubin 1990). It can be useful to observe some of these infrared lines even in optically *unobscured* sources such as planetary nebulae, where they enable one to measure additional ions of particular elements (Dinerstein 1980; Pottasch et al. 1986). At longer wavelengths there is the useful line trio of [O III] 52, 88 μm, and [N III] 57 μm. We have already discussed some uses of the first pair (Section II). Addition of the 57 μm line provides a measurement of N^{++} / O^{++} which is relatively independent of local conditions, because the critical densities of all three lines are similar (Moorwood et al. 1980; Dinerstein 1986). Observations of these lines in H II regions ranging from the Galactic Center to outside the solar circle indicate elevated values of N/O in the inner Galaxy, although the behavior is not necessarily a simple linear gradient (Lester et al. 1987).

Another type of "invisible" region is gas that is too cool to excite strong line emission in optical/uv transitions, for example gas with extremely high abundances of coolants such as O, N, and S. Such material can be found in gas processed by explosive nucleosynthesis, in supernova remnants and the ejecta of classical novae. When the densities become low enough that the ground state fine-structure lines are not collisionally suppressed, the gas cools extremely efficiently through these lines and the temperature plummets from of order 10,000 K to below 1000 K, causing the optical/uv lines to disappear. Such an "infrared

catastrophe" has been predicted to occur in evolving nova ejecta, shifting the main radiative cooling from the optical/uv into the far-infrared lines (Itoh 1981a; Ferland et al. 1984). However, such infrared lines have not yet been directly seen. IRAS saw broad-band infrared emission from several old novae (Dinerstein 1986b), but it has not yet been possible to demonstrate whether these fluxes are due to lines or to thermal emission from dust because of their faintness. Likewise, pure-metal inclusions in old supernova remnants should emit strongly in infrared lines from their constituent elements (Itoh 1981b, c; Dopita, Binette, & Tuohy 1984). Although there is some tantalizing evidence for lines from Gas A (Dinerstein et al. 1987), the presence of a strong thermal continuum from heated dust makes the lines harder to detect (Dwek et al. 1987).

Significant overabundances of particular species can produce strong infrared emission lines in novae and supernovae even while the ejecta are relatively hot. For example, the extremely strong 12.8 μm [Ne II] line seen in QU Vul led to the designation of a new class of novae, the "neon novae" (Gehrz, Grasdalen, & Hackwell 1985). Overabundances of Ne, Si, Mg, and other nearby elements are taken as evidence that this class of novae represents thermonuclear explosions on the surfaces of massive, O-Ne-Mg white dwarfs rather than C-O white dwarfs. An advantage of infrared lines is that they can be seen even if dust condenses in the ejecta, creating internal extinction that can hamper observations of ultraviolet emission lines. The first direct demonstration that Type Ia supernovae produce large amounts of iron was the observation of the 1.64 μm [Fe II] emission line in SN 1983n in M83 (Graham et al. 1986). Some further discussion of abundances in supernovae follows in Section 3.3.

4.2. Ionic abundance ratios

One nagging issue in the use of infrared lines to measure abundance ratios has been the discrepancy between the derived values and values determined from other methods. (I have previously called this the "zero point" issue.) An acute example has been the difference between N/O ratios determined from the far-infrared [O III], [N III] lines and values determined *for the same objects* from optical lines of [O II] and [N II]. As of several years ago, the infrared determinations of N/O for optically visible H II regions like Orion and M17 were yielding values two to three times higher than the optically determined values (Simpson et al. 1986; Lester et al. 1987).

Various possibilities were proposed as being responsible for this uncomfortable situation. First, does the problem lie in translating from line intensities to ionic abundances? The infrared lines are relatively insensitive to temperature, and their density dependence is well compensated for by deriving the density from the far-infrared [O III] lines; furthermore, the density "bias" introduced by clumping is minimal for this particular line set (Rubin 1989). On the other hand, the optical lines *are* temperature-sensitive, and furthermore the [O II] lines may be enhanced by dielectric recombination, causing the [N II] / [O II] line ratio to yield too low a value (Rubin 1986). Another possibility lies in the translation from the ionic ratio N^{++} / O^{++} to the elemental ratio, N/O. Rubin et al. (1988) advocated application of a correction factor for the relative volumes of N^{++} and O^{++}, which begin to decouple at stellar temperatures cooler than about 37,000 K. However, their correction factors are based on the fractional volume of these ionization zones integrated over the entire nebula, and therefore substantially overestimate the effect for H II regions that are much larger than the instrument beam used to make the observations, which has been the case for most of the far-infrared observations to date. Furthermore, most of the luminous H II regions studied in the galactic gradient surveys are probably ionized by stars hotter than 37,000 K, except for those close to the Galactic Center.

Finally, the discrepancy might be attributed to the use of incorrect atomic constants, especially collision strengths. Accurate atomic parameters for the far-infrared [O III] have been available for a decade (e.g., Aggarwal 1983), but the value of the [57 μm] collision strength, which is crucial for the ionic ratio, has been uncertain. During the late 1980's, an older value (Nussbaumer & Storey 1979) was replaced by a higher, unpublished value (Butler & Storey 1986). However, the latter has now been superceded by a still larger value, about twice the original one (Blum & Pradhan 1992). This new value lowers the Orion N^{++} / O^{++} ratio to 0.27, which is not far from the recent optical redetermination from N^{+} / O^{+} of 0.23 (Baldwin et al. 1991). Furthermore, when the new collision strength is applied to planetary nebulae with hot central stars, there is no longer any evidence for a systematic difference between N/O determined from the infrared and the optical lines (Dinerstein et al. 1995a, b).

4.3. Altered & evolving abundances

Infrared lines can provide evidence for the destruction of dust grains and the subsequent liberation of atoms, enhancing the gas-phase abundances of refractory elements relative to their usual depleted values in the interstellar medium. Such an effect may be responsible for the observed strength of near-infrared [Fe II] lines in supernova remnants, as discussed in Section 3.3. A similar effect is seen in the 35 μm [Si II] line in the Galactic Center region (Herter et al. 1989) and in shocked material in Orion (Haas, Hollenbach, & Erickson 1991).

A more exotic situation occurs in supernovae, where actual elemental abundances can change with time due to radioactive decay. In particular, the decay chain of ^{56}Ni -> ^{56}Co -> ^{56}Fe can be tracked through infrared lines. The first indication that this sequence might be observable was the identification of a feature at 10.5 μm in SN 1987A as being due to [Co II] rather than [S IV] (Rank et al. 1988). At shorter wavelengths, spectral monitoring of SN 1987A revealed a dramatic effect: the decay of a [Co

II] line and simultaneous growth of an adjacent [Fe II] feature at 1.54 μm (see Fig. 8, from Varani et al. 1990). Nickel was also seen in SN 1987A via [Ni II] lines at 6.63 μm (Wooden et al. 1993) and elsewhere. The spectral region 15-30 μm contains lines of all three elements, Ni, Co, and Fe, and many of these were seen in SN 1987A (Moseley et al. 1989). If the physics of the expanding supernova envelope is sufficiently well understood, or the local conditions can be strongly constrained by diagnostic line ratios, these line strengths can be used to deduce the manufactured masses of these elements. A less dramatic but still important probe of supernova physics is the use of the strong near-infrared He I lines at 1.08, 2.06 μm, which may be the most sensitive indicators of trace amounts of He in a supernova, as, for example, in SN 1993J in M81 (Swartz et al. 1993).

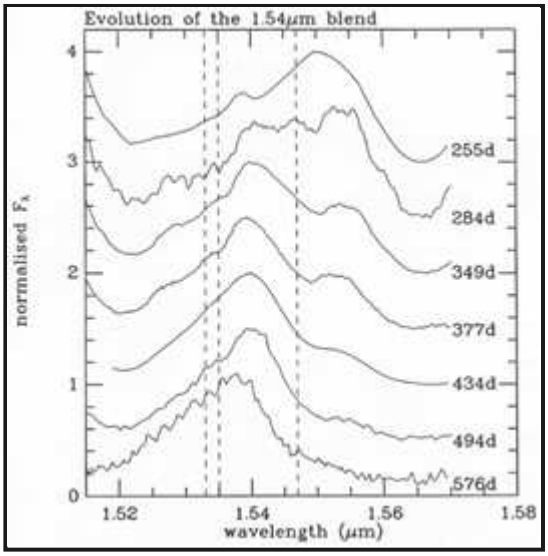

Figure 8. Evolution of the spectrum of SN 1987A . The vertical dashed lines indicate, from left to right, the wavelengths of [Fe II] 1.533 μm, [Fe I] 1.535 μm, and [Co II] 1.547 μm. Note the dramatic shift of the line peak as the cobalt decays into iron. (From Varani et al. 1990)

5. SOME CURRENT ISSUES: A SAMPLER

5.1. The origin of strong [Fe II] lines

One of the issues currently inspiring much discussion and gnashing of teeth is the origin of the very strong [Fe II] lines in some sources, particularly compared with their H I or H_2 emission. We have already touched on this question in the context of supernova remnants, where it is unclear whether the line strengths require actual grain destruction and/or gas-phase enrichment of the iron from SN debris, or whether the presence of a deep, partially ionized zone (caused either by shocks or by power-law photoionization) is sufficient (see Section 3.3). At the Galactic Center, the [Fe II]/H I line ratios are intermediate between those for H II regions and SNRs (DePoy 1992).

In spatially unresolved sources such as starbursts in galaxies and AGN's, there is a slightly different "[Fe II] conundrum." Even if we do not fully understand the cause of the strong [Fe II] emission in SNRs, a number of investigators have assumed that it is reasonable to consider such emission to be a tracer of the presence of SNRs. The case for a strong link between SNRs and the infrared [Fe II] lines is supported by the spatial correlation of [Fe II] emission with SN remnants in M82 (Greenhouse et al. 1991). Additional input to this issue comes from observations of the near-infrared H_2 lines in Seyfert galaxies and starbursts. The ratios of the H_2 and the [Fe II] lines are generally taken as evidence for shocks (Forbes & Ward 1993), with more recent work apparently putting to rest earlier claims of "fluorescent" H_2 ratios (see Moorwood & Oliva 1990 for a discussion). However, the issue is far from completely settled (e.g., Mouri, Kawara, & Taniguchi 1993). For example, there may be a shock without SNRs, for example a large-scale wind shock driven by an active nucleus (Kawara, Nishida, & Taniguchi 1988; Lester & Thompson 1990). Or possibly both the [Fe II] and H_2 lines are produced by photoionization, by a power-law continuum source rich in high-energy photons. Probably the strongest evidence for power-law ionization is observations of coronal lines such as [Si VI] 1.96 μm (Oliva & Moorwood 1990; Greenhouse et al. 1993).

5.2. Curiosities at the Galactic Center

The last few years have seen dramatic new developments in infrared spectroscopic studies of the Galactic Center. High velocity ($v \geq 500$ km s^{-1}) components in the 2.06 μm He I line, first detected over a decade ago (Hall, Kleinmann, & Scoville 1982), were hard to understand as originating from the diffuse, low-density ambient gas (Geballe et al. 1991). A new point of view, which has emerged from recent high spatial resolution spectroscopic mapping, is that these lines arise in the stellar winds of a cluster of hot, exotic, mass-losing objects akin to Wolf-Rayet stars (Krabbe et al. 1991). The UV radiation from these stars ionizes the adjacent material, but the stellar winds also drive fast shocks into the adjacent material, producing a hot, wind-swept "cavity" (Lutz, Krabbe, & Genzel 1993). The conditions in this cavity produce a variety of [Fe III] lines, whose ratios constrain the temperature and density of the gas (see their Fig. 6). The extent to which this cluster of hot stars is a paradigm for the central regions of other galaxies is unclear, but it does provide a sobering reminder that the Galactic Center is a special environment which may host many different kinds of unusual phenomena (and not "merely" black holes!).

5.3. Infrared spectroscopy of AGN

We have already mentioned infrared spectroscopy of AGN in the context of line intensity ratios of [Fe II], H I, and H_2. There are other interesting applications of infrared spectroscopy to AGN. One is to look at infrared H I lines in Seyfert 2 galaxies, where all the optical lines are relatively narrow, and search for a reddened broad-line component, or "buried" Seyfert 1 (e.g., Hines 1991). In the current paradigm of "unified" theories for AGN, such objects are viewed nearly "edge-on," so that the narrow-line gas (located farther from the central engine) is seen directly, whereas the inner, broad-line region is hidden by a dusty torus (e.g., Antonucci 1993). In the near-infrared the extinction is lower, so the broad-line region is more easily seen and therefore the broad wings become more apparent in the line profiles as one goes to longer and longer wavelengths. A second use of infrared spectroscopy is to observe the familiar "optical" lines, such as [O III] 5007 Å and Hα, in high-redshift objects (Hill, Thompson, & Elston 1993).

6. CONCLUDING REMARKS

This review has not, of course, covered every conceivable application of infrared spectroscopy. One major area I have omitted is the use of line velocities and profiles to study the kinematics and dynamics of astronomical sources. This type of study is not as unique to infrared lines as are some of the other topics discussed above, except in studying regions of heavy obscuration, such as the nuclei of starburst galaxies such as M82 (e.g., Achtermann & Lacy 1995). So far there has been only a limited amount of high-resolution infrared spectroscopy of emission lines, primarily due to sensitivity limitations. We can anticipate explosive growth of this area in the future, as infrared astronomers become less "signal-starved" with the advent of improved instruments and facilities. On the instrumentation side, individual detectors have already achieved high quantum efficiencies, but for spectroscopic applications, there is a tremendous advantage to using large detector arrays to obtain simultaneous coverage of a large number of spectral resolution elements.

The next decade will also see a major step forward in the light-gathering power of telescopes. On the ground, there will be several 8-10 m class telescopes in operation. Some of them more infrared-optimized than others, but all will undoubtedly be used for at least some infrared spectroscopy: Keck I & II and the Subaru Telescope, on Mauna Kea; Gemini North & South, in Hawaii & Chile; the VLT, in Chile, and the Hobby-Eberly Telescope in Texas. For spectral regions that are blocked from the ground, ESA's Infrared Space Observatory (ISO), scheduled to be launched in late 1995, will be the first space telescope to do extensive infrared spectroscopy. The premier facility for continuing infrared spectroscopic work at these wavelengths will be the Stratospheric Facility for Infrared Astronomy (SOFIA), a 3 m airborne telescope (Erickson & Davidson 1995). SOFIA's ten-fold increase in collecting area and smaller beam size, compared with the KAO, will give it the sensitivity to do infrared spectroscopy on relatively faint and distant sources, and its operational mode will encourage frequent upgrading of auxiliary instrumentation such as infrared spectrometers. At this writing, it appears likely that SOFIA will be in operation by around the year 2000. It is to be hoped that other, more advanced infrared space observatories, such as SIRTF, will follow soon after.

The utility of infrared emission line observations will also be improved by advances on the theoretical side. One major uncertainty in the interpretation of infrared lines has been the values of some of the atomic constants. Fortunately, this situation is now beginning to be remedied (e.g., Blum & Pradhan 1992). Improved models of the chemical, ionization, and thermal structure of photoionized regions, photodissociation regions, and interstellar shocks may help resolve some of the present anomalies and discrepancies that have arisen from studies of infrared emission lines, and permit stronger conclusions to be drawn on the roles of shocks and photoionization in distant galaxies.

Infrared spectroscopy is rapidly becoming a tool that is used by a large number of astronomers, rather than being the domain of a specialized few. This is likely to become even more true in the future, when facility infrared spectrometers on large telescopes are readily available to guest observers without specialized training. Thus, it is useful for all of us to be aware of the potential of infrared emission lines for nebular astrophysics. The techniques reviewed in this paper are merely the beginning of the harvest to be reaped from infrared line spectroscopy in the future.

I am grateful to the organizers of this conference for giving me the opportunity to present this review and to participate in this very special occasion, honoring two scientists who have played such a major role in advancing our understanding of the properties and physics of nebulae. I also wish to acknowledge research support from NSF grant AST 91-15101 and HST grant GO 3880.01-91A during the preparation of this review.

REFERENCES

1. ACHTERMANN, J. M., & LACY, J. H. 1995 *ApJ* **439**, 163.
2. AGGARWAL, K. M. 1983 *ApJS* **52**, 387.
3. ALLER, L. H. 1984 *Physics of Thermal Gaseous Nebulae* (Dordrecht: Reidel).
4. ANTONUCCI, R. 1993 *ARAA* **31**, 473.
5. ASHLEY, M. C. B., & HYLAND, A. R. 1988 *ApJ* **331**, 532.
6. BALDWIN, J. A., FERLANDS, G. F., MARTIN, P. G., CORBIN, M. R., COTA, S. A., PETERSON, B. M., & SLETTEBAK, A. 1991 *ApJ* **374**, 580.
7. BALDWIN, J. A., PHILLIPS, M. M., & TERLEVICH, R. 1981 *PASP* **93**, 5.
8. BENJAMIN, R. A., & DINERSTEIN, H. L. 1990 *AJ* **100**, 1588.
9. BLACK, J. H., & DALGARNO, A. 1976 *ApJ* **203**, 132.
10. BLACK, J. H., & VAN DISHOECK, E. F. 1987 *ApJ* **322**, 412.
11. BLUM, R. D., & PRADHAN, A. K. 1992 *ApJS* **80**, 425.
12. BRAND, P. W. J. L., MOORHOUSE, A., BURTON, M. G., GEBALLE, T. R., BIRD, M., & WADE, R. 1988 *ApJ* **334**, L103.
13. BURTON, M. G., HOLLENBACH, D. J., & TIELENS, A. G. G. M. 1990 *ApJ* **365**, 620.
14. BUTLER, K., & STOREY, P. J. 1986 private communication.
15. CARRAL, P., HOLLENBACH, D. J., LORD, S. D., COLGAN, S. W. J., HAAS, M. R., RUBIN, R. H., & ERICKSON, E. F. 1994 *ApJ* **423**, 223.
16. COLGAN, S. W. J., HAAS, M. R., ERICKSON, E. F., RUBIN, R. H., SIMPSON, J. P., & RUSSELL, R. W. 1993 *ApJ* **413**, 237.
17. DEPOY, D. L. 1992 *ApJ* **398**, 512.
18. DINERSTEIN, H. L. 1980 *ApJ* **237**, 486.
19. DINERSTEIN, H. L. 1983 in *Planetary Nebulae, IAU Symposium 103* (ed. D. R. Flower) Dordrecht: Reidel, 79.
20. DINERSTEIN, H. L. 1986a *PASP* **98**, 979.
21. DINERSTEIN, H. L. 1986b *AJ* **92**, 1381.
22. DINERSTEIN, H. L. 1990 in *The Interstellar Medium in Galaxies* (eds. H. A. Thronson, Jr. & J. M. Shull) Dordrecht: Kluwer, 257.
23. DINERSTEIN, H. L., & BENJAMIN, R. A. 1993 *RevMexA&A* **27**, 33.
24. DINERSTEIN, H. L., HAAS, M. R., ERICKSON, E. F., & WERNER, M. W. 1995a in the *Airborne Astronomy Symposium on the Galactic Ecosystem: From Gas to Stars to Dust* (eds. M. R. Haas, J. A. Davidson, & E. F. Erickson) ASP Conference Series, vol. 73, in press.
25. DINERSTEIN, H. L., HAAS, M. R., ERICKSON, E. F., & WERNER, M. W. 1995b in preparation.
26. DINERSTEIN, H. L., LESTER, D. F., CARR, J. S., & HARVEY, P. M. 1988 *ApJ* **327**, L27.
27. DINERSTEIN, H. L., LESTER, D. F., RANK, D. M., WERNER, M. W., & WOODEN, D. H. 1987 *ApJ* **312**, 314.
28. DOPITA, M. A., BINETTE, L., & TUOHY, I. R. 1984 *ApJ* **282**, 142.
29. DRAINE, B. T. 1980 *ApJ* **241**, 1021.
30. DRAINE, B. T., & MCKEE, C. F. 1993 *ARAA* **31**, 373.
31. DRAINE, B. T., ROBERGE, W. G., & DALGARNO, A. 1983 *ApJ* **264**, 485.
32. DWEK, E., DINERSTEIN, H. L., GILLETT, F. C., HAUSER, M. G., & RICE, W. L. 1987 *ApJ* **315**, 571.
33. ERICKSON, E. F., & DAVIDSON, J. A. 1995 in the *Airborne Astronomy Symposium on the Galactic Ecosystem: From Gas to Stars to Dust* (eds. M. R. Haas, J. A. Davidson, & E. F. Erickson) ASP Conference Series, vol. 73, in press.
34. EVANS, I. N. & DOPITA, M. A. 1985 *ApJS* **58**, 125.
35. FERLAND, G. J., WILLIAMS, R. E., LAMBERT, D. L., SHIELDS, G. A., SLOVAK, M., GONDHALEKAR, P. M., & TRURAN, J. W. 1984 *ApJ* **281**, 194.
36. FORBES, D. A., & WARD, M. J. 1993 *ApJ* **416**, 150.
37. GATLEY, I., et al. 1987 *ApJ* **318**, L73.
38. GEBALLE, T. R., KRISCIUNAS, K., BAILEY, J. A., & WADE, R. 1991 *ApJ* **370**, L73.
39. GEBALLE, T. R., PERSSON, S. E., SIMON, T., LONSDALE, C. J., & MCGREGOR, P. J. 1986 *ApJ* **302**, 693.
40. GEHRZ, R. D. 1988 *ARAA* **26**, 377.
41. GEHRZ, R. D., GRASDALEN, G. L., & HACKWELL, J. A. 1985 *ApJ* **298**, L47; **306**, L49.
42. GOODRICH, R. W. 1990 *ApJ* **355**, 88.
43. GRAHAM, J. R., MEIKLE, W. P. S., ALLEN, D. A., LONGMORE, A. J., & WILLIAMS, P. M. 1986 *MNRAS* **218**, 93.
44. GRAHAM, J. R., WRIGHT, G. S., & LONGMORE, A. J. 1987 *ApJ* **313**, 847.

45. GRAHAM, J. R., WRIGHT, G. S., & LONGMORE, A. J. 1990 *ApJ* **352**, 172.
46. GRAHAM, J. R., WRIGHT, G. S., HESTER, J. J., & LONGMORE, A. J. 1991 *AJ* **101**, 175.
47. GRASDALEN, G. L., & JOYCE, R. R. 1976 *Nature* **259**, 187.
48. GREENHOUSE, M. A., FELDMAN, U., SMITH, H. A., KLAPISCH, M., BHATIA, A. K., & BARSHALOM, A. 1993 *ApJS* **88**, 23.
49. GREENHOUSE, M. A., GRASDALEN, G. L., WOODWARD, C. E., BENSON, J., GEHRZ, R. D., ROSENTHAL, E., & SKRUTSKIE, M. F. 1990 *ApJ* **352** 307.
50. GREENHOUSE, M. A., WOODWARD, C. E., THRONSON, H. A., RUDY, R. J., ROSSANO, G. S., ERWIN, P., & PUETTER, R. C. 1991 *ApJ* **383**, 164.
51. HAAS, M. R., HOLLENBACH, D., & ERICKSON, E. F. 1991 *ApJ* **374**, 555.
52. HASEGAWA, T., GATLEY, I., GARDEN, R. P., BRAND, P. W. L., OHISHI, M., HAYASHI, M., & KAIFU, N. 1987 *ApJ* **318**, L77.
53. HAYASHI, M., HASEGAWA, T., GATLEY, I., GARDEN, R., & KAIFU, N. 1985 *MNRAS* **215**, 31P.
54. HERTER, T., HELFER, H. L., & PIPHER, J. L. 1983 *A&AS* **51**, 195.
55. HERTER, T., GULL, G. E., MEGEATH, S. T., ROWLANDS, N., & HOUCK, J. R. 1989 *ApJ* **343**, 696.
56. HILL, G. J., THOMPSON, T. L., & ELSTON, R. 1993 *ApJ* **414**, L1.
57. HINES, D. C. 1991 *ApJ* **374**, L9.
58. HOLLENBACH, D. J., & MCKEE, C. F. 1989 *ApJ* **342**, 306.
59. HOLLENBACH, D. J., TAKAHASHI, T., & TIELENS, A. G. G. M. 1991 *ApJ* **377**, 192.
60. ITOH, H. 1981a *PASJ* **33**, 743.
61. ITOH, H. 1981b *PASJ* **33**, 1.
62. ITOH, H. 1981c *PASJ* **33**, 521.
63. KAWARA, K., NISHIDA, M., & PHILLIPS, M. M. 1989 *ApJ* **337**, 230.
64. KAWARA, K., NISHIDA, M., & TANIGUCHI, Y. 1988 *ApJ* **328**, L41.
65. KEENAN, F. P. & CONLON, E. S. 1993 *ApJ* **410**, 426.
66. KEENAN, F. P., BURKE, V. M., & AGGARWAL, K. M. 1991 *ApJ* **371**, 636.
67. KRABBE, A., GENZEL, R., DRAPATZ, S., & ROTACIUC, V. 1991 *ApJ* **382**, L19.
68. LATTER, W. B., MALONEY, P. R., KELLY, D. M., BLACK, J. H., RIEKE, G. H., & RIEKE, M. J. 1992 *ApJ* **389**, 347.
69. LESTER, D. F., CARR, J. S., JOY, M., & GAFFNEY, N. 1990 *ApJ* **352**, 544.
70. LESTER, D. F., DINERSTEIN, H. L., & RANK, D. M. 1979 *ApJ* **229**, 981.
71. LESTER, D. F., DINERSTEIN, H. L., WERNER, M. W., WATSON, D. M., GENZEL, R., & STOREY, J. W. V. 1987 *ApJ* **320**, 573.
72. LESTER, D. F., & THOMPSON, K. L. 1990 *ApJ* **348**, L49.
73. LUHMAN, M. L., JAFFE, D. T., KELLER, K. D., & PAK, S. 1994 *ApJ* **436**, L185.
74. LUTZ, D., KRABBE, A., & GENZEL, R. 1993 *ApJ* **418**, 244.
75. MATHIS, J. S. 1990 *ARAA* **28**, 37.
76. MCKEE, C. F., CHERNOFF, D. F., & HOLLENBACH, D. J. 1984 in *Galactic & Extragalactic Infrared Spectroscopy* (eds. M. F. Kessler & J. P. Phillips) Dordrecht: Reidel, 103.
77. MOORWOOD, A. F. M., BALUTEAU, J.-P., ANDEREGG, M., CORON, N., BIRAUD, Y., & FITTON, B. 1980 *ApJ* **238**, 565.
78. MOORWOOD, A. F. M., & OLIVA, E. 1990 *A&A* **239**, 78.
79. MOURI, H., KAWARA, K., & TANIGUCHI, Y. 1993 *ApJ* **406**, 52.
80. MOSELEY, S. H., DWEK, E., GLACCUM, W., GRAHAM, J. R., LOEWENSTEIN, R. F., & SILVERBERG, R. F. 1989 *ApJ* **347**, 1119.
81. NATTA, A., GIOVANARDI, C., PALLA, F., & EVANS, N. J. II 1988 *ApJ* **327**, 817.
82. NUSSBAUMER, H., & STOREY, P. J. 1979 *A&A* **71**, L5.
83. NUSSBAUMER, H., & STOREY, P. J. 1988 *A&A* **193**, 327.
84. OLIVA, E., & MOORWOOD, A. F. M. 1990 *ApJ* **348**, L5.
85. OLIVA, E., MOORWOOD, A. F. M., & DANZIGER, I. J. 1989 *A&A* **214**, 307.
86. OLIVA, E., MOORWOOD, A. F. M., & DANZIGER, I. J. 1990 *A&A* **240**, 453.
87. OSTERBROCK, D. E. 1988 *PASP* **100**, 412.
88. OSTERBROCK, D. E. 1989 *Astrophysics of Gaseous Nebulae and Active Galactic Nuclei* (Mill Valley, CA: University Science Books).
89. OSTERBROCK, D. E., TRAN, H. D., & VEILLEUX, S. 1992 *ApJ* **389**, 196.
90. PEIMBERT, M. 1967 *ApJ* **150**, 825.
91. PEIMBERT, M. 1993 *RevMexA&A* **27**, 9.
92. PEIMBERT, M. & COSTERO, R. 1969 *Bol. Obs. Tonantzintla y Tacubaya* **5**, 3.
93. POTTASCH, S. R., PREITE-MARTINEZ, A., OLNON, F. M., RAIMOND, E., BEINTEMA, D. A., & HABING, H. J. 1985 *A&A* **143**, L11.
94. POTTASCH, S. R., PREITE-MARTINEZ, A., OLNON, F. M., MO, J.-E., & KINGMA, S. 1986 *A&A* **161**, 363.

95. RAMSAY, S. K., CHRYSOSTOMOU, A., GEBALLE, T. R., BRAND, P. W. J. L., & MOUNTAIN, M. 1993 *MNRAS* **263**, 695.
96. RANK, D. M., DINERSTEIN, H. L., LESTER, D. F., BREGMAN, J. D., AITKEN, D. K., & JONES, B. 1978 *MNRAS* **185**, 179.
97. RANK, D. M., PINTO, P. A., WOOSLEY, S. E., BREGMAN, J. D., WITTEBORN, F. C., AXELROD, T. S., & COHEN, M. 1988 *Nature* **331**, 505.
98. ROWLANDS, N., HOUCK, J. R., HERTER, T., GULL, G. E., & SKRUTSKIE, M. F. 1989 *ApJ* **341**, 901.
99. RUBIN, R. 1989 *ApJS* **69**, 897.
100. RUBIN, R. 1985 *ApJS* **57**, 349.
101. RUBIN, R. H., SIMPSON, J. P., ERICKSON, E. F., & HAAS, M. R. 1988 *ApJ* **327**, 377.
102. RUBIN, R., SIMPSON, J. P., HAAS, M. R., & ERICKSON, E. F. 1991 *ApJ* **374**, 564.
103. SEARLE, L. 1971 *ApJ* **165**, 259.
104. SEATON, M. J. & OSTERBROCK D. E. 1957 *ApJ* **125**, 66.
105. SELLGREN, K. 1986 *ApJ* **305**, 399.
106. SHIELDS, J. C. 1993 *ApJ* **419**, 181.
107. SHULL, J. M., & DRAINE, B. T. 1987 in *Interstellar Processes* (eds. D. J. Hollenbach & H. A. Thronson) Dordrecht: Reidel, 283.
108. SHURE, M. A., HERTER, T., HOUCK, J. R., BRIOTTA, D. A., JR., FORREST, W. J., GULL, G. E., & MCCARTHY, J. F. 1983a *ApJ* **270**, 645.
109. SHURE, M. A., HERTER, T., & HOUCK, J. R. 1983b *ApJ* **274**, 646.
110. SIMPSON, J. P. 1975 *A&A* **39**, 43.
111. SIMPSON, J. P. 1984 *ApJ* **281**, 184.
112. SIMPSON, J. P., RUBIN, R. H., ERICKSON, E. F., & HAAS, M. R. 1986 *ApJ* **311**, 895.
113. SIMPSON, J. P., & RUBIN, R. 1990 *ApJ* **354**, 165.
114. SPINOGLIO, L., & MALKAN, M. A. 1992 *ApJ* **399**, 504.
115. STERNBERG, A., & DALGARNO, A. 1989 *ApJ* **338**, 197.
116. SWARTZ, D. A., CLOCCHIATTI, A., BENJAMIN, R., LESTER, D. F., & WHEELER, J. C. 1993 *Nature* **365**, 232.
117. THOMPSON, R. I. 1982 *ApJ* **257**, 171.
118. TIELENS, A. G. G. M. & HOLLENBACH, D. 1985 *ApJ* **291**, 722 (TH).
119. VARANI, G.-F., MEIKLE, W. P. S., SPYROMILIO, J., & ALLEN, D. A. 1990 *MNRAS* **245**, 570.
120. VOIT, G. M. 1992 *ApJ* **399**, 495.
121. WATSON, D. M. 1985 *Phys. Scripta* **T11**, 33.
122. WILLIAMS, R. E. 1991 in *IAU Colloquium 122, Physics of Classical Novae* (eds. A. Cassatella & R. Viotti) Berlin: Springer, 215.
123. WOLFIRE, M. G., TIELENS, A. G. G. M., & HOLLENBACH, D. J. 1990 *ApJ* **358**, 116.
124. WOODEN, D. H., RANK, D. M., BREGMAN, J. D., WITTEBORN, F. C., TIELENS, A. G. G. M., COHEN, M., PINTO, P. A., & AXELROD, T. S. 1993 *ApJS* **88**, 477.